Spin Freezing and Magnetic Inhomogeneities in Bilayer Manganites

A. I. Coldea,[1] S. J. Blundell,[1] C. A. Steer,[1] J. F. Mitchell,[2] and F. L. Pratt[3]

[1]*Clarendon Laboratory, University of Oxford, Parks Road, Oxford OX1 3PU, United Kingdom*
[2]*Materials Science Division, Argonne National Laboratory, Argonne, Illinois 60439*
[3]*Rutherford Appleton Laboratory, Chilton, Didcot OX11 0QX, United Kingdom*

We have performed a muon spin rotation study on polycrystalline samples of electron-doped layered manganites, $La_{2-2x}Sr_{1+2x}Mn_2O_7$ ($0.4 \leq x < 1$), in order to investigate the local magnetic structure and spin dynamics. Our results provide evidence for phase separation into A-type antiferromagnetic and charge-ordered phases for $x = 0.52$ and spin freezing at low temperatures ($T < 100$ K) for $0.52 \leq x < 0.75$. A new phase diagram which includes this spin-freezing region is proposed.

The phenomenon of phase separation is crucial for determining the intrinsic properties of many magnetic oxides [1]. The origin of the colossal magnetoresistance (CMR) in manganese perovskite structures is often linked to the coexistence of ferromagnetic (FM) metallic and antiferromagnetic charge-ordered (CO) insulating domains or to the formation of nanoscale magnetic clusters [2,3]. One technique which provides information on the local magnetic order is muon spin rotation/relaxation (μSR). In underdoped cuprates, μSR has identified the coexistence of superconducting and antiferromagnetic phases as well as spin freezing believed to be related to the generation of stripes [4].

In this Letter, we provide direct evidence for spin freezing and phase separation in electron-doped layered manganite structures using μSR. We investigate the local magnetic structure and spin dynamics across a series of magnetic structures of $La_{2-2x}Sr_{1+2x}Mn_2O_7$ with $0.4 \leq x < 1$. For compounds in the Mn^{4+}-rich half of the phase diagram ($0.5 < x < 1$), neutron diffraction studies [5] reveal a progression of antiferromagnetic (AFM) insulating phases: from A type ($0.5 \leq x < 0.66$) to C/C^* type ($0.75 \leq x < 0.9$) and to G type ($0.9 < x \leq 1.0$). Furthermore, no long-range magnetic order (NLRO) has been observed between the A-type AFM and C/C^*-type AFM regions ($x = 0.66$–0.74) [5]. Our experiments measure the temperature dependence of the order parameter in the samples with long-range order (LRO) and show how this is affected by the interplay between magnetic and charge order. Moreover, by cooling a sample in the NLRO region, we are able to follow the progressive slowing down of magnetic fluctuations and demonstrate the development of short-range order. Based on our results, we are able to propose a new phase diagram of $La_{2-2x}Sr_{1+2x}Mn_2O_7$ ($0.5 \leq x < 1$), supplementing the information already obtained from neutron diffraction [5].

Zero-field μSR is especially suited for study of short-range magnetic correlations since the positive muons are a sensitive local probe. Because the local magnetic fields at muon sites result primarily from dipolar interactions

which decay very quickly with increasing distance ($\sim 1/r^3$), the effective range investigated with muons is ~ 20 Å. In a system having magnetically ordered and disordered regions, the μSR data is composed of two different signals corresponding to different environments, with signal amplitudes roughly proportional to their volume fraction. In the case of a magnetically ordered system, our data are fitted using a relaxation function, $G_z(t)$, of the form

$$G_z(t) = A_{rlx} \exp(-t/T_1) + A_{osc} \cos(2\pi\nu_\mu t) \exp(-t/T_2),$$
(1)

where the first term is the longitudinal (spin-lattice) relaxation, the second term is the muon precession at frequency $\nu_\mu = \gamma_\mu B_\mu / 2\pi$ in the local internal field, B_μ, in the ordered state, $1/T_2$ is the transverse relaxation rate, and $\gamma_\mu/2\pi = 135.5$ MHz/T is the gyromagnetic ratio. The longitudinal relaxation rate is defined by $1/T_1 \propto (\gamma_\mu \Delta B_\mu)^2 \tau$ for rapid fluctuations, where ΔB_μ is the amplitude of the fluctuating field and τ is the Mn-ion correlation time. Near a magnetic phase transition τ (and, hence, $1/T_1$) increases with cooling due to the critical slowing down. For polycrystalline samples, where the local magnetization points along the muon spin direction with probability $1/3$, the corresponding amplitudes are $A_{rlx} = G_z(0)/3$ and $A_{osc} = 2G_z(0)/3$. Equation (1) can be generalized in a straightforward manner if there are multiple frequencies in the data corresponding to magnetically inequivalent sites. Polycrystalline samples (~ 0.5 g) were prepared as described in Ref. [6]. Zero-field μSR data for ten compositions were taken on the EMU beam line at the ISIS facility (Rutherford Appleton Laboratory, United Kingdom) and for five compositions on the GPS spectrometer at the PSI muon facility (Paul Scherrer Institute, Switzerland).

Figure 1 shows μSR spectra collected at $T = 1.8$ K (at PSI). Two oscillations can be distinguished for the G-type AFM sample, $x = 0.98$, and only one damped oscillation for all others, although for $x = 0.68$ the damping is
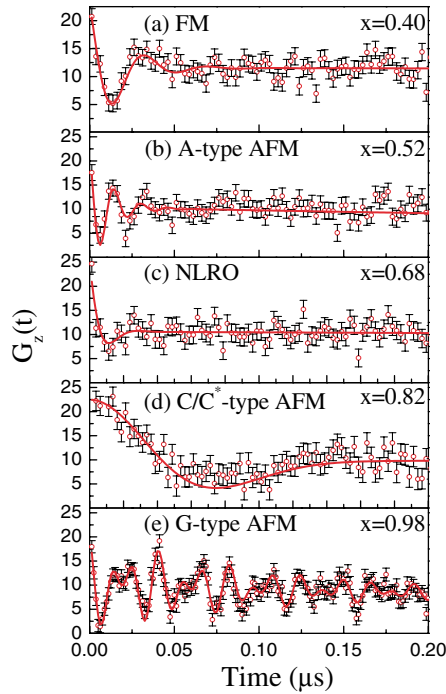
FIG. 1 (color online). Muon spin relaxation data at $T = 1.8$ K for La$_{2-2x}$Sr$_{1+2x}$Mn$_2$O$_7$ with (a) $x = 0.40$ (FM), (b) $x = 0.52$ (A-type AFM), (c) $x = 0.68$ (NLRO), (d) $x = 0.82$ (C/C*-type AFM), and (e) $x = 0.98$ (G-type AFM). Two oscillation frequencies can be observed for $x = 0.98$ and a very strongly damped oscillation for $x = 0.68$. The solid lines are fits to the data using Eq. (1).

extremely large. The data were fitted using Eq. (1) and the obtained parameters are listed in Table I. The source of the internal field is attributed to the aligned manganese moments in the vicinity of the muon. As a function of hole doping, x, the values of ν_μ indicate changes in the local field when the spin structure varies. The precession frequency for $x = 0.40$ is $\nu_\mu = 28(1)$ MHz at $T = 1.8$ K [which corresponds to an internal field of $B_\mu = 0.21(1)$ T], similar to that found for the ferromagnetic system, $x = 0.3$ [7]. The observation of two muon frequencies for the G-type AFM compound, $x = 0.98$, suggests that the muon occupies magnetically inequivalent sites in this compound. In oxides the muon site is usually

TABLE I. Parameters obtained by fitting the μSR spectra for La$_{2-2x}$Sr$_{1+2x}$Mn$_2$O$_7$ at 1.8 K (Fig. 1).

Sample	ν_μ (MHz)	$1/T_2$ (μs^{-1})	$1/T_1$ (μs^{-1})	$1/(2\pi\nu_\mu T_2)$ (%)
$x = 0.40$	28(1)	57(6)	0.005(1)	0.32(4)
$x = 0.52$	68(4)	110(14)	0.10(1)	0.26(4)
$x = 0.68$	30(5)	150(23)	0.06(2)	0.80(18)
$x = 0.82$	5.4(2)	20(1)	0.03(1)	0.58(15)
$x = 0.98$	47(2)/76(2)	16(2)	0.065	0.054/0.034(0.6)

about 1 Å from an oxygen atom [8]. In the layered manganite structure there are three inequivalent oxygen sites O(1), O(2), and O(3), and one likely muon site is close to O(2) (0, 0, 0.2) [7].

The longitudinal relaxation rate, $1/T_1$, at $T = 1.8$ K is 2–3 orders of magnitude smaller than the transverse relaxation rate, $1/T_2$, indicating that the relaxation of oscillations is dominated by a *static* distribution of internal local fields determined by the neighboring Mn spins at the muon site [9]. Nevertheless, some *dynamic* broadening, i.e., fluctuations of Mn spins, is also present since $1/T_1$ is nonzero. The relative width of the field distribution can be parametrized by $1/(2\pi\nu_\mu T_2)$ (Table I) which is very large (≈ 0.80) for the NLRO sample ($x = 0.68$) and quite small (< 0.055) for the G-type AFM compound ($x = 0.98$) that has only 2% Mn^{3+} ions mixed with Mn^{4+} ions. A large relative width can be associated with a large distribution of Mn^{3+} and Mn^{4+} ions (resulting in a large degree of local magnetic inhomogeneity), or with the coexistence of different magnetic phases.

The temperature dependence of $\nu_\mu(T)$ [and, hence, $B_\mu(T)$] for $x = 0.52$ and $x = 0.98$ is shown in Fig. 2. For $x = 0.52$, we find a discontinuity in $\nu_\mu(T)$ around 100 K. This arises because of the presence of two magnetic phases, A-type AFM and a CO phase similar to that found in $x = 0.5$ [10,11], which compete with each other
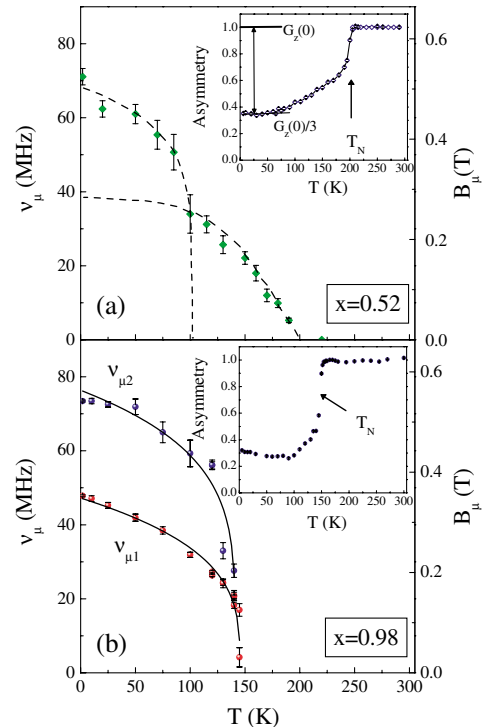

FIG. 2 (color online). Temperature dependence of the zero-field muon precession frequency, ν_μ, and internal field, B_μ, for (a) $x = 0.52$ and (b) $x = 0.98$. The inset shows the temperature dependence of the relaxing asymmetry, A_{rlx} for the two compositions.

in the region between 100 and 200 K. Below 100 K, the internal field increases significantly due to an additional magnetic transition. This transition coincides with a broad maximum in $1/T_1$ [12], signifying a freezing of the local spins. This effect is strikingly similar to that observed in a bilayer cuprate [4], in which a *freezing* of spins of doped holes is superimposed on AFM long-range ordered Cu^{2+} spins. The slow variation of the relaxing asymmetry, A_{rlx} (inset of Fig. 2) between $G_z(0)$ (at 200 K) and $G_z(0)/3$ (below 100 K) further confirms the *two-phase model* whose volume fraction is temperature dependent, and that the whole sample is magnetic below 100 K. The behavior of the $x = 0.52$ compound is in contrast to the G-type AFM compound, $x = 0.98$, for which the drop in the initial asymmetry is much sharper [see inset of Fig. 2(b)] and both precession frequencies $\nu_{\mu 1}(T)$ and $\nu_{\mu 2}(T)$ can be fitted to $\nu_{\mu i}(T) = \nu_{\mu i}^0 (1 - T/T_N)^\beta$ [Fig. 2(b)]. This procedure, although usually applicable only to the asymptotic critical regime, gives a reasonable description of the data over the entire temperature range [see Fig. 2(b)], yielding $T_N = 145.0(5)$ K in agreement with neutron powder diffraction [5] and $\beta = 0.24(2)$ [close to the value corresponding to a 2D XY system ($\beta = 0.23$) [13,14]].

One of the most intriguing regions of the Mn^{4+}-rich phase diagram is $x = 0.66$–0.74, where NLRO has been detected using neutron diffraction [5]. Data for $x = 0.68$ at $T = 1.8$ K shown in Fig. 1(c) were analyzed using a relaxation function which was (i) Eq. (1) for $T \leq 70$ K, (ii) $G_z(t) = A_s e^{-\lambda_s t} + A_f e^{-\lambda_f t}$ for 70 K $< T \leq 120$ K, and (iii) $G_z(t) = A_f e^{-\lambda_f t}$ for $T > 120$ K, and the results of the fitting are presented in Fig. 3. At low temperatures, the strongly damped oscillation frequency decreases upon warming from ~ 30 MHz at 2 K to ~ 10 MHz around 65 K [inset of Fig. 3(b)], suggesting the development of a quasistatic field at the muon site indicative of short-range order. In the low temperature regime, we found that modeling data using a Gaussian Kubo-Toyabe relaxation function parametrized by $\Delta_{KT}/(2\pi)$ gave similar results [see inset of Fig. 3(b)].

The broad static distribution of local fields is quantified by the large $1/T_2$ values which is replaced by the slow dynamic relaxation rate λ_s above 70 K [inset of Fig. 3(c)]. The damped oscillations disappear above 70 K, the temperature at which $1/T_1$ exhibits a pronounced maximum, corresponding to the slowing down of spin fluctuations, and we identify this temperature as the *spin-freezing* temperature, T_f. The amplitudes of the two components A_{osc} and A_{rlx} shown in Fig. 3(b) provide information about the volume fractions of the sample where muons experience static or dynamic spin-lattice relaxation, respectively. Above T_f, the oscillatory component A_{osc} (and the corresponding frequency ν_μ) disappears and is replaced by a slowly fluctuating fraction with amplitude A_s [Fig. 3(b)]. This fraction decreases upon heating above T_f and disappears around 120 K. At high temperatures, the
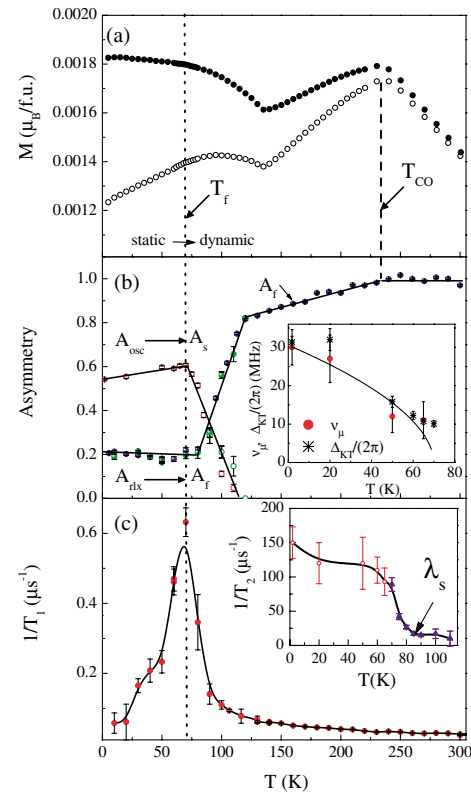

FIG. 3 (color online). Temperature dependence of different fitting parameters for $x = 0.68$; (a) the zero-field cooled (open circles) and field-cooled (closed circles) magnetization in 10 mT; (b) the static amplitude (A_{osc} for $T < T_f$ and A_s for $T > T_f$) and the dynamic amplitude (A_{rlx} for $T < T_f$ and A_f for $T > T_f$); inset shows $\nu_\mu(T)$ and $\Delta_{KT}/(2\pi)$; (c) longitudinal relaxation rate, $1/T_1$ (the inset shows the transverse relaxation rate, $1/T_2$, and slow component, λ_s). The freezing temperature T_f (vertical dotted line) separates the static and the dynamic regions. The vertical dashed line shows T_{CO} defined as the maximum in the magnetization data, in agreement with electron diffraction studies [15]. The solid lines are a guide to the eye.

main source of depolarization is the fast fluctuating spins and the corresponding volume fraction, A_f, increases linearly on warming (for 120 K $< T < T_{CO}$). This suggests that in this temperature range the short-range (CE-type) or dynamic CO dominates the muon depolarization, as found for $x = 0.5$ [16] and $La_{1-x}Ca_x MnO_3$ [17]. The zero-field-cooled magnetization decreases almost linearly with temperature for 120 K $< T < T_{CO}$ due to the formation of short-range antiferromagnetic correlations in the CO region [Fig. 3(a)].

In the limit of fast fluctuations, one can estimate the correlation time, τ, of magnetic fluctuations by assuming that the static width of the field distribution is of the order of the average magnetic field sensed by muons at the lowest temperature ($\gamma_\mu \Delta B_\mu \sim 2\pi \nu_\mu$). We estimate short correlation times associated with fast fluctuations in the range $\tau_f = 10^{-12}$–10^{-13} s for all samples, in good
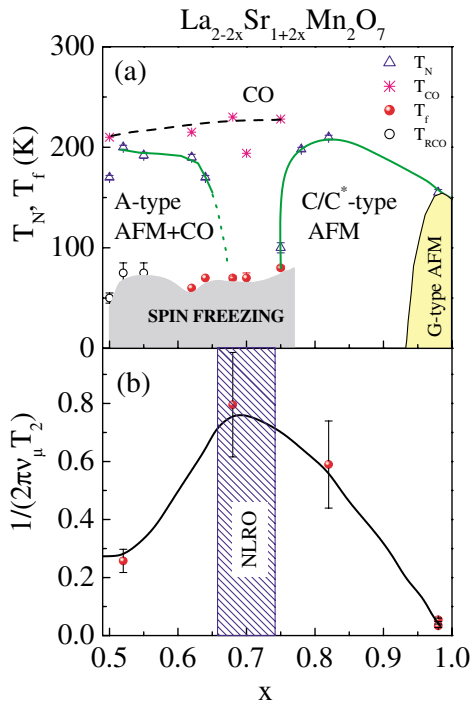
FIG. 4 (color online). (a) Phase diagram of $La_{2-2x}Sr_{1+2x}Mn_2O_7$ ($0.5 < x < 1$). The charge ordering temperatures were obtained from magnetization data [12]. Solid and dashed lines are guides to the eye. (b) Degree of magnetic inhomogeneity at 1.8 K expressed by $1/(2\pi\nu_\mu T_2)$.

agreement with other values reported for bilayer manganites [18,19]. For $x = 0.68$, the additional slowly fluctuating component observed between 70 and 120 K fluctuates with a correlation time $\tau_s = 10^{-9}$–10^{-11} s. The existence of *slow* and *fast* dynamics between $T_f < T < 120$ K for $x = 0.68$ further sustains the *phase separation* scenario in which charge-ordered and ferromagnetic (or *A*-type or *C*-type AFM) regions may coexist in the NLRO region, as found in $La_{1-x}Ca_xMnO_3$ [20].

The freezing mechanism begins with the formation of magnetic clusters at high temperatures. Thermal disorder opposes this tendency, so that with decreasing temperature the regions of correlated spins become larger and the spin system is subdivided into independent magnetic clusters of different size with a distribution of blocking temperatures. If a cluster is blocked for a time greater than the time window of the μSR technique, it will appear *frozen* or *quasistatic* and, hence, A_{rlx} decrease reflects a progressive blocking of clusters by cooling down towards T_f, where all clusters are blocked. Spin-freezing phenomena are found in numerous systems, ranging from spin glasses, such as Cu-Mn alloys [21] to lightly doped cuprates, $La_{2-x}Sr_xCuO_4$ [4]. In our layered manganites, we find that short-range charge-ordered fluctuations are *dynamic* at high temperatures ($T < T_{CO}$) and become *static* below T_f (or in the reentrant charge-ordered region). We note that there has been evidence for spin

freezing in manganese perovskites ascribed to magnetic cluster formation and/or magnetic polarons [22,23] or stripelike structures [24].

In conclusion, our μSR study of electron-doped bilayer manganites yields *local* magnetic information and provides evidence for magnetic order, phase separation, and *spin freezing*. The results are summarized in the phase diagram shown in Fig. 4(a). Spin freezing is observed as a maximum in $1/T_1$ for samples with $x = 0.52$–0.75 [12]. The spin frozen state thus exists in the region of the phase diagram with LRO ($x = 0.52$–0.62) together with a LRO state (AFM for $x = 0.52$) and also in the region for which neutron diffraction failed to detect any LRO. We note that the *spin-frozen* region of the phase diagram overlaps closely with a region in which *reentrant charge ordering* has been suggested to exist [11,15,25,26]. We can quantify the degree of local magnetic inhomogeneity at low temperatures using $1/(2\pi\nu_\mu T_2)$ [Fig. 4(b)] which is largest for the $x = 0.68$ composition in the NLRO region [5].

[1] E. Dagotto *et al.*, Phys. Rep. **244**, 1 (2001).
[2] M. Uehara *et al.*, Nature (London) **399**, 560 (1999).
[3] J. M. De Teresa *et al.*, Nature (London) **386**, 256 (1997).
[4] C. Niedermayer *et al.*, Phys. Rev. Lett. **80**, 3843 (1998).
[5] C. D. Ling *et al.*, Phys. Rev. B **62**, 15096 (2000).
[6] J. E. Millburn *et al.*, Chem. Commun. **15**, 1389 (1999).
[7] R. H. Heffner *et al.*, Phys. Rev. Lett. **81**, 1706 (1998).
[8] J. H. Brewer *et al.*, Hyperfine Interact. **63**, 177 (1990).
[9] $1/T_1$ was also extracted over $\Delta t = 0.1$–25 μs.
[10] D. N. Argyriou *et al.*, Phys. Rev. B **61**, 15269 (2000).
[11] T. Chatterji *et al.*, Phys. Rev. B **61**, 570 (2000).
[12] A. I. Coldea, Ph.D. thesis, Oxford University, 2001.
[13] S. T. Bramwell *et al.* J. Phys. Condens. Matter **5**, L53 (1993).
[14] S. Rosenkranz *et al.*, Physica (Amsterdam) **312B–313B**, 763 (2002).
[15] J. Q. Li *et al.*, Phys. Rev. B **64**, 174413 (2001).
[16] D. Andreica *et al.*, Physica (Amsterdam) **289B–290B**, 65 (2002).
[17] K. H. Kim *et al.*, Phys. Rev. B **62**, R11 945 (2000).
[18] T. G. Perring *et al.*, Phys. Rev. Lett. **78**, 3197 (1997).
[19] J.-W. Feng *et al.*, Phys. Rev. B **63**, 180401 (2001).
[20] R. H. Heffner *et al.*, Phys. Rev. B **63**, 094408 (2001).
[21] A. W. Hunt *et al.*, Phys. Rev. Lett. **82**, 4300 (1999).
[22] G. Papavassiliou *et al.*, Phys. Rev. Lett. **87**, 177204 (2001).
[23] G. Allodi *et al.*, Phys. Rev. Lett. **87**, 127206 (2001).
[24] T. Hotta, Phys. Rev. Lett. **86**, 4922 (2001).
[25] Q. Yuan *et al.*, Phys. Rev. Lett. **83**, 3502 (1999).
[26] J. Dho *et al.*, J. Phys. Condens. Matter **13**, 3655 (2001).